

# Spontaneous Fractal Spatial Pattern Formation

Jungang Huang and G.S. McDonald

Joule Physics Laboratory, School of Computing, Science and Engineering,  
Institute of Materials Research, University of Salford, Salford M5 4WT, UK

We report a generic mechanism for spontaneous fractal spatial pattern formation, believing this to be the first such report. The mechanism has independence with respect to both the particular form of non-linearity and the particular context of the non-linear system. From our simulation we know that this system can generate a scale-dependent fractal. In the one-dimensional case its fractal dimension changes from 2 to 1 with increase in spatial frequency.

## Introduction

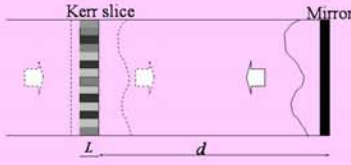
Complexity focuses on commonality across subject areas and forms a natural platform for multidisciplinary activities. Typical generic signatures of complexity include: (i) spontaneous occurrence of simple pattern (e.g. stripes, hexagons), emerging as a dominant non-linear mode, and (ii) formation of highly complex pattern in the form of a fractal (with structure spanning decades of scale). However, to our knowledge, a firm connection between these two signatures has not previously been established. This is perhaps not surprising since system non-linearity tends to impose a specific scale, while fractals are defined by their scale-less character.

In the photonics domain, Berry [1] established that fractal light may be generated in simple LINEAR optical systems. More recently, the highly-structured (linear) modes of unstable-cavity lasers were discovered to be fractal in character [2], and optical fractal generators based upon introducing electronic feedback/non-linearity have also been developed [3]. Instead, we propose intrinsic non-linear dynamics providing both the necessary feedback mechanism and the pattern seed for building fractals.

## Kerr-slice-with-single-feedback-mirror System

The system, as showed in the figure below, is composed of a thin slice of Kerr medium illuminated from one side by a spatially smooth beam and a feedback mirror a distance  $d$  away to generate counter-propagating beams in the Kerr slice [4]. The reflectivity of the mirror is  $R$ . The photoexcitation density  $n$  of the Kerr medium has a relaxation time constant  $\tau$  and a diffusion length  $l_D$ . To simplify the numerical model, the thickness  $L$  of the Kerr medium is considered to be small enough so that the time by which light transverses though it and the diffraction caused by it can both be neglected. Then the evolution of the system can be represented by the following equations:

$$\frac{\partial F}{\partial z} = i\chi n F, \quad \frac{\partial B}{\partial z} = -i\chi n B$$

$$-l_D^2 \nabla_{\perp}^2 n + \tau \frac{\partial n}{\partial t} + n = |F + B|^2$$


where  $\chi$  parameterizes the Kerr effect (positive for a focusing medium, negative for a defocusing medium), and  $F$  and  $B$  are the forward and backward field respectively.

According to free space propagation, the Fourier transforms of the forward and backward fields obey the relation:

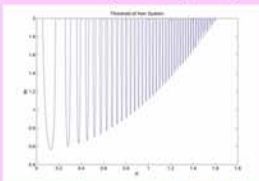
$$B(K) = e^{-i\theta} F(K) \quad \theta = \frac{2d}{k_0} \frac{K^2}{1 + \sqrt{1 - \frac{K^2}{k_0^2}}}$$

where  $B(K)$  and  $F(K)$  are the Fourier transforms of the backward and forward fields, and  $k_0$  is the wave number of the beam. From this equation, we know that any frequency components higher than  $k_0$  will die out after propagation. So one can also use  $k_0$  to control the maximum frequency which can pass through the free space.

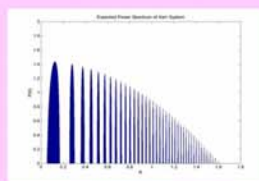
## Pattern Formation Thresholds

From linear stability analysis [4], the instability threshold of the system is:

$$|\chi| IL = \frac{1 + K^2 l_D^2}{2(R + \sqrt{R}) |\sin(K^2 d / k_0)|}$$



(2a) Threshold ( $d/k_0 = 100, l_D = 1, R = 0.9, \chi L = 1$ )



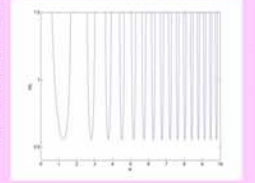
(2b) Expected spectrum

This threshold divides the frequency space into an infinite number of frequency bands. Their widths and the separations between nearby bands decrease with  $K$ . The lowest threshold values in the bands increase smoothly with  $K$ .

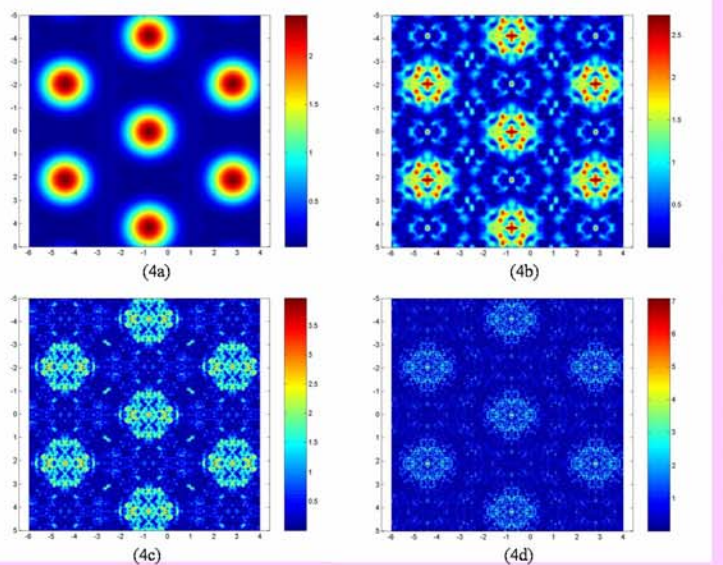
Naturally, we expect the power spectrum of the pattern to be proportional to the difference between the input wave spectrum and the threshold. Comparing the expected spectrum of the Kerr system with the spectra of unstable laser modes [5], the amplitudes both decrease smoothly by some laws with increase in frequency, though these laws are different.

We therefore hope that this system can also generate optical fractals.

The figure on the right is the threshold plot for  $l_D=0, \tau=0, d/k_0=1$ , and  $R=0.9$ . The lowest threshold of each frequency band is equal. So if we make the intensity of the incident plane wave slightly higher than the lowest threshold, the frequencies with the same lowest threshold in all bands will have the same growth rate. The intensity distribution in a two-dimensional plane is then an extremely complex pattern with a fractal dimension of 3.



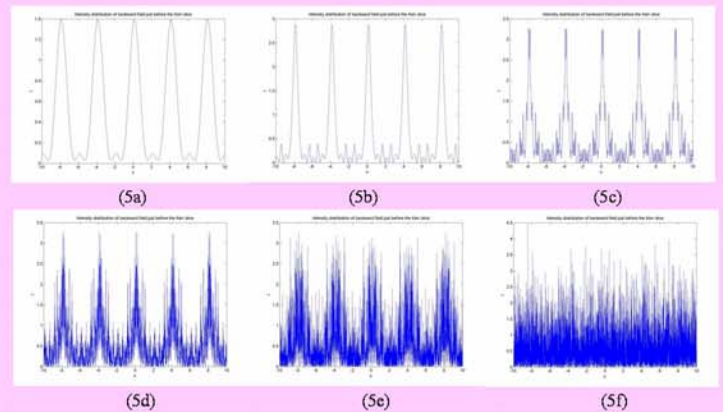
## Spontaneous Optical Fractals



Two-dimensional pattern evolution of the system when  $l_D=0, \tau=0, d/k_0=1$ , and  $R=0.9$ . (4a) has a one-band-pass frequency filter imposed. (4b), (4c) and (4d) are patterns after the filter is removed. (4b)  $t=3T_R$ , (4c)  $t=6T_R$ , (4d)  $t=9T_R$  ( $T_R=2d/c$ ,  $c$  is the speed of light).

We introduce a filter by setting  $k_0$  so that only frequencies in the first band can pass. We start with plane-wave input and steady-state photoexcitation density plus a small white noise of 1%. The backward field intensity distribution becomes the static hexagonal pattern shown in figure (4a). We then instantly open up the filter (set  $k_0$  to infinity) to see how the system evolves. Three intermediate patterns are shown in figures (4b), (4c) and (4d). Pattern evolution is from hexagon towards a fractal pattern with a fractal dimension of 3.

## Pattern Evolution in Time: $l_D=0$

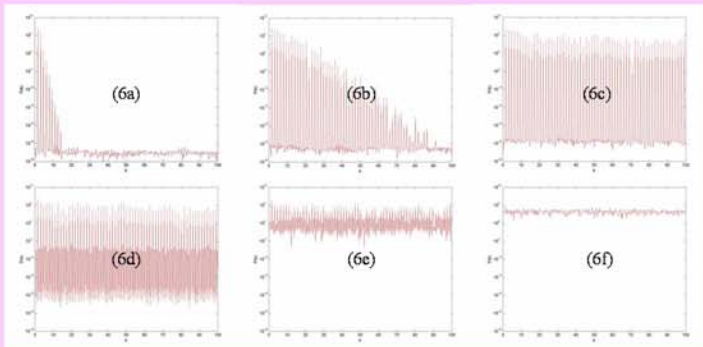


Pattern evolution in time when  $l_D=0, \tau=0, d/k_0=1$ , and  $R=0.9$ . (5a) has a one-band-pass frequency filter imposed (5b) through to (5f) are patterns after the filter is removed. (5b)  $t=2T_R$ , (5c)  $t=7T_R$ , (5d)  $t=13T_R$ , (5e)  $t=16T_R$ , (5f)  $t=50T_R$  ( $T_R=2d/c$ ,  $c$  is the speed of light).

We also simulate the system with just one transverse dimension. The pattern evolution of the backward field from a simple one to a fractal-like one is shown in figure 5, and the corresponding power spectra are plotted in figure 6. Figure (5a) is the pattern formed under the same conditions as the pattern shown in figure (4a).



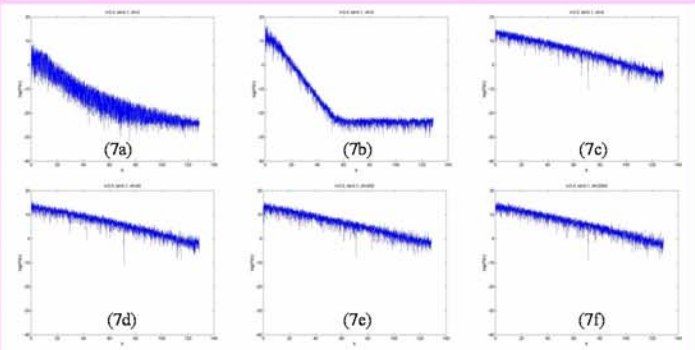
## Power Spectrum Evolution in Time: $I_D=0$



Power spectrum evolution in time when  $I_D=0$ ,  $\tau=0$ ,  $d/k_0=1$ , and  $R=0.9$  (6a) has a one-band-pass frequency filter imposed (6b) through to (6f) are patterns after the filter is removed. (b)  $t=2T_R$ , (c)  $t=7T_R$ , (d)  $t=13T_R$ , (e)  $t=16T_R$ , (f)  $t=50T_R$  ( $T_R=2d/c$ ,  $c$  is the speed of light).

The harmonic frequencies of the dominant frequency grow more rapidly than other frequency components, and those with lower frequency grow more rapidly. After  $50T_R$ , all frequency components reach a value with the same order of magnitude. We can consider the fractal pattern of this system as composed of an infinite number of simple patterns of different size.

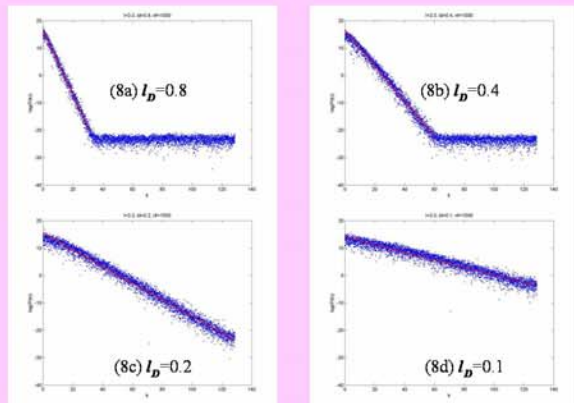
## Power Spectrum Evolution in Time: $I_D=0.1$



Power spectrum evolution in time when  $I_D=0.1$ ,  $d/k_0=100$ ,  $R=0.9$ ,  $\chi L=1$ , and  $I_m=3.0$ . (a)  $t=2T_R$ , (b)  $t=5T_R$ , (c)  $t=10T_R$ , (d)  $t=50T_R$ , (e)  $t=500T_R$ , (f)  $t=2000T_R$  ( $T_R=2d/c$ ,  $c$  is the speed of light).

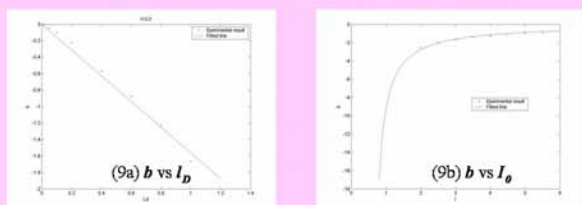
These figures show the dynamic evolution when medium diffusion is included. The speed of the process does change with system parameters, such as the intensity of the incident wave. But fractal formation is nonetheless very fast, typically less than  $50T_R$ . Figures (7d), (7e) and (7f) show that the logarithm of the power spectrum normally distributes around a straight line. While the evolution of the system continues to redistribute power in the different space frequencies, this does not change either the intercept or the slope of the line around which the power is distributed.

## Spectrum Variation with Diffusion ( $I_D$ )



The red lines in figures (8a), (8b), (8c) and (8d) are calculated by linear regression. The slopes of the lines increase with decrease of the diffusion length.

## Summary of Power Law Characteristics



Variation of the slope  $b$  of the line of trend versus (a) diffusion length  $I_D$  and (b) intensity of incident plane wave  $I_0$ . (a)  $I_0=3.0$ ,  $d/k_0=100$ ,  $R=0.9$  and  $\chi L=1$ . (b)  $I_D=1.0$ ,  $d/k_0=100$ ,  $R=0.9$  and  $\chi L=1$ .

The slope is found to vary linearly with  $I_D$ . Figure (9b) shows the relation between slope  $b$  and intensity of input wave  $I_0$ . The line fitted has the equation  $b=b_0 I_0 / (I_0 - I_m)$ , where  $I_m$  is the lowest threshold for pattern formation and  $b_0$  is a constant.

The average trend of the logarithm of the power spectrum can be represented by a straight line. That is:

$$\log(P(k)) = a + bk$$

Where  $P(k)$  and  $k$  are the power spectrum and space frequency, respectively, and  $a$  and  $b$  are constants dictated by system parameters. Then, we have:

$$\frac{d(\ln P)}{d(\ln k)} = bk$$

Using  $D = \frac{1}{2} + \frac{1}{2} \frac{d(\ln P)}{d(\ln k)}$ , one obtains an expression of power spectrum fractal dimension:

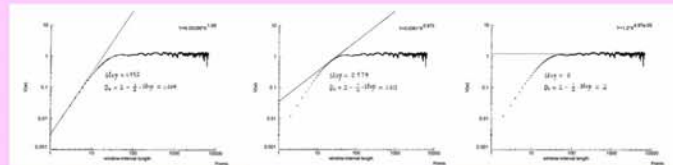
$$D(k) = \frac{5}{2} + \frac{b}{2}k$$

For our one-dimensional calculations,  $D$  must be between 1 and 2. So the equation of the fractal dimension should be written as:

$$D(k) = \begin{cases} 2 & D(k) > 2 \\ \frac{5}{2} + \frac{b}{2}k & 1 \leq D(k) \leq 2 \\ 1 & D(k) < 1 \end{cases} \quad \text{when}$$

Since  $D$  varies with  $k$  (in common with unstable laser modes), we refer to the patterns generated by this system as *scale-dependent fractals*.

## Fractal Dimension vs. $k$

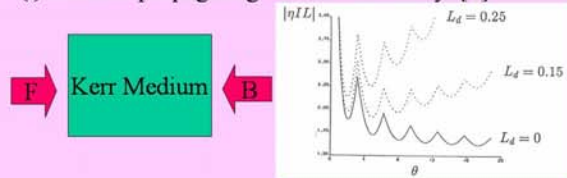


The above plot is obtained by using Benoit 1.3 [8]. Benoit appears to be one of the most popular software in fractal analysis. One can see that the slope of the tangent decrease smoothly from 2 to 0 when the window interval length increases from 1 to 100; the average slope remains 0 when the window interval length is larger than 100. So, according to the definition of variogram fractal dimension,  $D=2-\text{slope}/2$ , the fractal dimension increases from 1 to 2 when the window interval length increases from 1 to 100. It has a value of 2 when the window interval length is larger than 100.

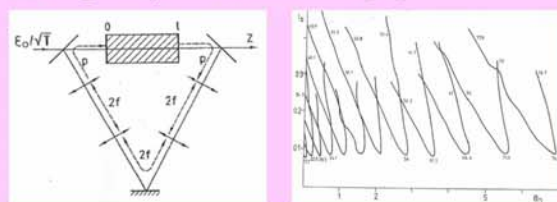
The fractal dimension of the pattern thus decreases smoothly from 2 to 1 with increase in spatial frequency. This result is consistent with that found by using the power spectrum method, and this proves our claim regarding the fractal dimension of the pattern.

## Other Nonlinear Systems

(i) Counter-propagating beams—no cavity [9]



(ii) Ring cavity with 2-level atoms [10]



## Conclusions

- ❖ The first prediction of spontaneous fractal pattern formation in an all-optical nonlinear system has been presented. Moreover, we identify this as a generic process that would arise in a wide variety of non-linear optical systems.
- ❖ The particularly simple system studied here generates optical fractals whose smallest scale is limited by either: (a) the optical wavelength, or (b) diffusion of the medium photoexcitation.
- ❖ Inclusion of a spatial filter has allowed us to demonstrate both conventional (single frequency) pattern formation and fractal formation in the same optical system.
- ❖ In the diffusion-limited system, we show that the dependence of spectral characteristics on the carrier diffusion length and the input pump intensity is given by a rather simple law.
- ❖ An analytical form is also derived for the (scale-dependent) fractal dimension, and predictions are confirmed by variogram analysis.

## References

- [1] M.V. Berry, I. Marzoli, W. Schleich, *Physics World* (June, 2001), 39.
- [2] G.P. Karman, G.S. McDonald, G.H.C. New, J.P. Woerdman, *Nature* 402 (1999) 138.
- [3] J. Courtial, J. Leach, M. J. Padgett, *Nature* 414 (2001) 864.
- [4] W. J. Firth, *J. Mod. Opt.* 37 (1991) 151.
- [5] M Berry, C Storm, W.V. Saarloos, *Opt. Commun.* 197 (2001) 393-402.
- [6] G. D'Alessandro, W. J. Firth, *Phys. Rev. Lett.* 66 (1991) 2597.
- [7] G Evans, J Blackledge, P Yardley, *Numerical methods for partial differential equations*, Springer, New York, 1999.
- [8] Benoit1.3, TruSoft International Inc.
- [9] W. J. Firth, *C. Pire, Opt. Lett.* 13 (1988) 1096.
- [10] A.S. Patrascu, C. Nath, M. Le Berre, E. Ressayre, A. Tallet, *Opt. Commun.* 91 (1992).